

Estimation of Circumferential Fiber Shortening Velocity by Echocardiography

DAVID G. RUSCHHAUPT, MD, PETER C. SODT, MD, NANCY A. HUTCHEON, BA,
RENE A. ARCILLA, MD, FACC

Chicago, Illinois

The M-mode and two-dimensional echocardiograms of 40 young patients were analyzed to compare the mean circumferential fiber shortening velocity (Vcf) of the left ventricle calculated separately by two methods. The mean circumferential fiber shortening velocity was derived from the M-mode echocardiogram as minor axis shortening/ejection time and derived from the two-dimensional echocardiogram as actual circumference change/ejection time. With computer assistance, circumference was determined from the short-axis two-dimensional echocardiographic images during end-diastole and end-systole. Good correlations were obtained between the left ventricular diameter derived by M-mode echocardiography and the vertical axis during end-diastole ($r = 0.79$) and

end-systole ($r = 0.88$) derived by two-dimensional echocardiography. Likewise, high correlations were noted between diameter and circumference in end-diastole ($r = 0.89$) and end-systole ($r = 0.88$). However, comparison of Vcf obtained by M-mode echocardiography with that obtained by two-dimensional echocardiography showed only fair correlation ($r = 0.68$). Moreover, the diameter/circumference ratio determined in end-diastole and end-systole differed significantly ($p < 0.001$), possibly owing to the change in geometry of the ventricular sector image during systole. Although Vcf derived by M-mode echocardiography is a useful index of left ventricular performance, it does not truly reflect the circumference change during systole.

The left ventricular contractile state can be quantified in human beings by relating instantaneous velocity of fiber shortening at the minor equator to the maximal wall tension during ejection (1). Because this type of analysis is very cumbersome, requiring high fidelity pressure recordings and high quality angiograms for frame by frame measurement of ventricular dimensions, it has remained only a research tool. Instead, simpler angiographic indexes of ventricular pump function, such as ejection fraction or mean velocity of circumferential fiber shortening (Vcf), have been widely used. In recent years, mean Vcf has been routinely measured in M-mode echocardiograms, taking into consideration the systolic change in left ventricular minor axis and the ejection time (2). The reliability of this noninvasive procedure for differentiating normal from abnormal left ven-

tricular performance was validated by Cooper et al. (3), who demonstrated good correlation between mean Vcf determined angiographically and that obtained by the ultrasound technique. However, it remains to be proven whether the Vcf derived from the echocardiogram indeed evaluates the changes in left ventricular circumference during systole. Our study was designed to test the validity of this echocardiographic tool as a measure of circumferential shortening velocity.

Methods

Study group. Forty young patients, 0.05 to 18.5 years of age, underwent M-mode and two-dimensional echocardiography. Thirteen had a normal heart, 9 had left ventricular pressure overload, 11 had left ventricular volume overload and 7 had primary myocardial disease. None had cardiac arrhythmia, bundle branch block or left ventricular asynergy, and none were in clinical cardiac failure at the time of study.

M-mode echocardiography. The M-mode echocardiograms were obtained using a Hoffrel 201 ultrasonoscope interfaced to a Honeywell 1856 strip chart recorder run at

From the University of Chicago, Pritzker School of Medicine, Department of Pediatrics, Section of Pediatric Cardiology, Chicago, Illinois. This study was supported by a grant (RR-305) from the General Clinical Research Centers Program of the Division of Research Resources, National Institutes of Health, Bethesda, Maryland. Manuscript received November 30, 1982; revised manuscript received February 1, 1983; accepted February 9, 1983.

Address for reprints: Rene A. Arcilla, MD, University of Chicago, 950 East 59th Street, Box 154, Chicago, Illinois 60637

a paper speed of 50 or 75 mm/s. The patients were in a nonsedated resting state in the supine position. Two transducers (Aerotech) were used: a 5.0 MHz, 0.6 cm diameter, nonfocused transducer for the infants and very young children, and a 3.5 MHz, 1.25 cm diameter, nonfocused transducer for the older patients. Full ultrasound recordings, including a lead II electrocardiogram showing a dominant R wave, were obtained using conventional techniques with the transducer generally positioned in the third left parasternal space (4-6).

Left ventricular dimensions were obtained from the tracings recorded as the ultrasound beam traversed the tip of the anterior mitral leaflet. The ventricular diameters during end-diastole (LVEDD) and end-systole (LVESD) were measured from the opposing endocardial echoes of the septum and posterior wall. Ventricular end-diastole was timed by the peak of the R wave of the electrocardiogram. Ventricular end-systole was temporally identified by the peak anterior excursion of the left ventricular posterior wall. The aortic root echoes were obtained by angling the ultrasound beam from the mitral valve toward the aortic root, and adjusting the transducer orientation until clear aortic valve echoes were recorded (7). Left ventricular ejection time (LVET) was measured from the time the aortic valve opened to the time it closed. All measurements were obtained from 3 to 5 consecutive cardiac cycles using a Hewlett-Packard digitizer (model 9874A) interfaced with a Hewlett-Packard computer (model 9845B).

Mean circumferential fiber shortening velocity (Vcf) was derived by the standard equation:

$$Vcf \text{ (circ/s)} = \frac{LVEDD - LVESD}{LVEDD \times LVET}$$

Two-dimensional echocardiography. The two-dimensional echocardiograms were obtained immediately after the M-mode study, with the patient supine and at rest. A commercially available phased array, wide angle sector scanner (Toshiba SSH-10A) with a 32 element, 2.4 MHz transducer was used. The displayed sector scan consisted of 112 lines that radiated from a point source on a cathode ray oscilloscope screen on which images appeared in real time at 30 frames/s with 1 cm calibration marks. Recordings were made in the conventional long-axis, short-axis, apical four-chamber and subxiphoid projections (8). The longitudinal or long-axis sector scan was obtained with the plane of the ultrasound beam parallel to the long axis of the left ventricle. The sector image included right ventricular outflow tract, aortic root, left atrium and basal portion of the left ventricle including both leaflets of the mitral valve. After recording the long-axis sector image, the transducer was rotated approximately 90° to obtain a transverse or short-axis image of the left ventricle. After a brief sweep from the apex

toward the base of the heart, the ultrasound beam was oriented toward the level of the mitral leaflet-chordal transition. A sector image of the left ventricular cross section was then recorded.

The two-dimensional images were recorded on 3/4 inch (1.9 cm) videotape, using an NEC video-cassette recorder (model 7505) for redisplay and evaluation in real time, slow motion format. In addition, a line-voltage synchronized 35 mm movie camera focused onto a slave monitor (Setchell Carlson) and simultaneously recorded the sector images at a film exposure rate of 30 frames/s, similar to the sector scanning rate. The cine films were analyzed using a Vanguard XR 35 projector, and critical images of the left ventricle were quantified using the same Hewlett-Packard digitizer computer.

Heart rate was derived from the number of frames separating consecutive QRS complexes of the simultaneously recorded lead II electrocardiogram (number of frames \times 33 ms = RR interval). Although subject to error because of the limited sector scanning rate, left ventricular ejection time was also estimated on the basis of the number of frames exposed while the aortic valve remained open as viewed in the long-axis plane. Ventricular end-diastole was identified by the peak of the R wave or its ascending limb. In the short-axis projection, the cine frame immediately preceding the opening of the mitral valve was designated as taken at end-systole.

Analysis of sector images. The cine films in the short-axis view were reviewed. Sector images showing portions of the left atrium during systole were not included in the analysis because this indicated incorrect (too cephalad) orientation of the transducer. The end-diastolic and end-systolic cine frames showing the entire left ventricular cross section were identified by their frame numbers, and the endocardial echoes abutting the left ventricular cavity were traced on paper. As in angiocardigraphic methods for estimating ventricular volume, minor irregularities of the ventricular surface were ignored. The position of the mitral valve echoes and the 1 cm calibration marks were also traced. When portions of the endocardium could not be readily identified in the stop-frame mode, slow playback of the contraction or filling patterns enhanced recognition of the endocardial targets. All tracings were obtained by the same person.

The border of the traced left ventricular image was slowly digitized, requiring 2 to 3 minutes to measure its circumference. Each cine image was digitized twice and the average of the duplicate measurements used. An on-line computer calculated circumference as the sum of tiny straight line segments averaging 0.84 mm in length. (The range of distance allowed between two consecutive points sampled was 0.6 to 1.2 mm.) All sampled distances were automatically corrected for magnification. With circles used as reference figures, the error of the method was no greater than 0.5%.

A transverse line parallel to the plane of the mitral valve and transecting a point midway between the anterior and posterior endocardial surfaces was drawn (horizontal axis). Another line perpendicular to the latter and also transecting the same point was drawn (vertical axis). Both axes were measured and corrected for magnification.

Reproducibility was tested by two means. One determined the variability of the circumference determination by quadruplicate measurements of 20 sector images. Interobserver variability was also tested using 10 other patients of whom 4 had grossly reduced left ventricular function. Two independent observers derived the end-diastolic and end-systolic circumferences without knowledge of the specific cine frames used by the other in the analysis.

Results

Representative cross-sectional images of the left ventricle in the short-axis view, reproduced from the 35 mm movie film, are shown in Figure 1. A slight change in ventricular geometry was usually observed during the cardiac cycle—from a somewhat oval shape during diastole to a relatively circular shape during systole. The extent of the geometric change varied from patient to patient and was unrelated to the underlying cardiac disease.

Reproducibility and interobserver variability. Analysis of variance in the quadruplicate measurements revealed a standard deviation of 0.97% from the mean circumference. Interobserver variability is summarized in Table 1. The average difference between the end-diastolic circumference calculations by the two observers was 2.4% of the mean circumference (range 0.3 to 5.6). The average difference between the end-systolic measurements was 2.6% of the mean circumference (range 0.3 to 10.5). The circumference change during systole was related to the end-diastolic circumference and expressed as percent of the latter. The av-

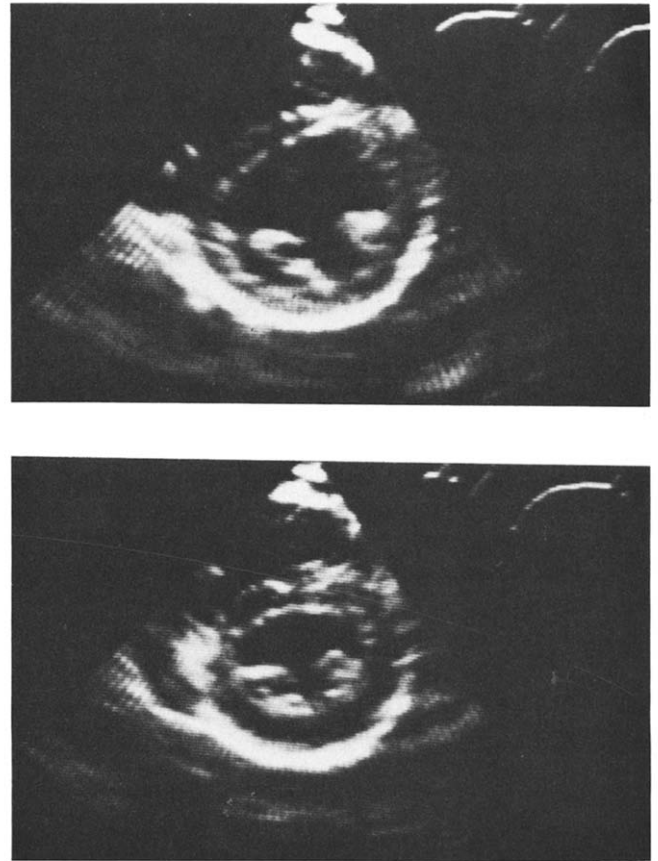


Figure 1. Sector images of the left ventricle in the short-axis view obtained during end-diastole (top) and end-systole (bottom) in a 10 year old child with a functional murmur.

erage difference between calculated circumference change by the two observers was 6.0% (range 0 to 11.8).

Heart rates and ejection times. The heart rates during the M-mode study were similar to those during the two-

Table 1. Interobserver Variability of Circumference Determinations in 10 Subjects

Case	End-diastolic Circumference (EDC) (cm)			End-systolic Circumference (ESC) (cm)			EDC-ESC/EDC		
	A	B	Δ	A	B	Δ	A	B	Δ
1	9.44	9.98	5.6%	6.41	7.12	10.5%	0.32	0.29	9.7%
2	9.93	9.71	2.2%	7.34	7.08	3.6%	0.26	0.27	3.8%
3	12.10	11.95	1.3%	7.65	7.43	2.9%	0.37	0.38	2.7%
4	12.50	12.55	0.4%	10.07	10.04	0.3%	0.19	0.20	5.1%
5	12.72	12.42	2.4%	11.02	10.93	0.8%	0.13	0.12	8.0%
6	13.75	13.36	2.9%	9.44	9.02	4.6%	0.31	0.32	3.2%
7	13.85	13.65	1.5%	10.71	10.51	1.9%	0.23	0.23	0%
8	15.27	14.84	2.9%	9.38	9.35	0.3%	0.39	0.37	5.3%
9	17.88	17.15	4.2%	14.04	13.92	0.9%	0.21	0.19	10.0%
10	21.71	21.77	0.3%	20.49	20.41	0.4%	0.056	0.063	11.8%
Mean	13.92	13.74	2.37%	10.66	10.58	2.62%	0.247	0.243	5.96%
±SD	3.67	3.56	1.65%	4.08	4.03	3.15%	0.106	0.103	3.15%

A = Observer A; B = Observer B; Δ = difference, expressed as percent of the mean of values obtained by Observer A and Observer B; SD = standard deviation.

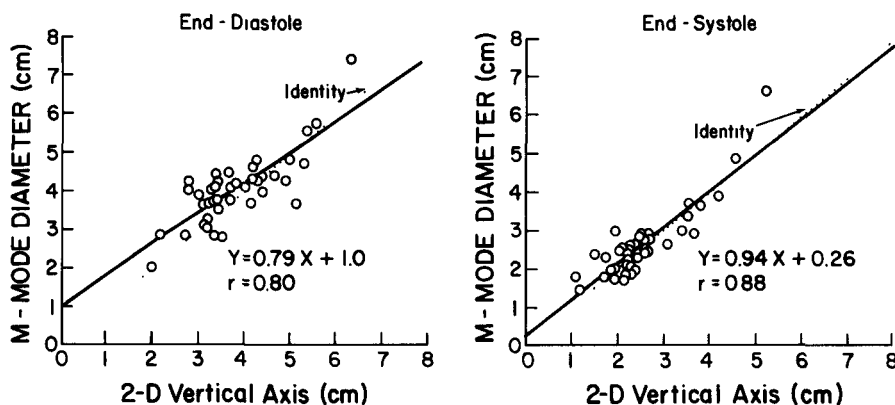


Figure 2. Comparison of left ventricular diameters obtained from M-mode echocardiograms with vertical axes derived from two-dimensional (2-D) echocardiograms during end-diastole and end-systole. Linear regression lines (solid) and lines of identity (dotted) are shown, as well as regression equations and correlation coefficients.

dimensional study. Mean M-mode heart rate \pm standard deviation was 86.6 ± 22 beats/min, compared with that (86.6 ± 23 , probability [p] = not significant [NS]) obtained during the two-dimensional study. In contrast, left ventricular ejection times measured from the M-mode tracing differed from those derived from the cine film. The average M-mode left ventricular ejection time was 0.264 ± 0.04 second; that obtained from the two-dimensional study was 0.292 ± 0.05 ($p < 0.001$ by paired *t* test). The difference in the left ventricular ejection time values by the two methods reflects the potential for errors and the limited sensitivity of two-dimensional echocardiograms, recorded at 30 frames/s, for timing short events in the cardiac cycle.

Left ventricular diameter and vertical axis. The left ventricular diameters obtained from the M-mode tracings correlated well with the vertical axes derived from the two-dimensional images (Fig. 2). The correlation coefficient was higher during end-systole ($r = 0.88$) than during end-diastole ($r = 0.80$). The regression line relating M-mode diameter to two-dimensional vertical axis in end-diastole differed from the line of identity ($p < 0.05$). In contrast, the end-systolic measurements by the two methods did not differ significantly. The M-mode end-diastolic diameter averaged 4.05 ± 0.93 cm as compared with the two-dimensional vertical axis of 3.82 ± 0.95 cm ($p < 0.025$ by paired

t test). Corresponding end-systolic values were 2.65 ± 0.93 and 2.56 ± 0.87 cm, respectively ($p = \text{NS}$).

Vertical axis and diameter related to circumference. The relation of the vertical axis of the sector image to its circumference was evaluated during end-diastole and end-systole. Excellent correlation was observed ($r = 0.88$ in end-diastole and $r = 0.92$ in end-systole). A plot of circumference as a function of vertical axis and the regression equations are shown in Figure 3. A similar relation was noted when circumference was related to the left ventricular diameter obtained from the M-mode tracings. The correlation coefficients during end-diastole and end-systole were 0.89 and 0.88, respectively (Fig. 4). The regression equations in Figure 4 did not statistically differ from the corresponding regression equations in Figure 3.

M-mode versus two-dimensional circumferential fiber shortening velocity (Vcf). Comparison of mean Vcf estimated from the M-mode echocardiograms with mean Vcf estimated from the two-dimensional echocardiograms revealed positive but only fair correlation (Fig. 5). This was equally observed when the left ventricular ejection time used to estimate the two-dimensional Vcf was that obtained from the M-mode tracing ($r = 0.68$), or when the left ventricular ejection time used was that derived from the cine film ($r = 0.62$). In either case, a plot of M-mode Vcf as a function

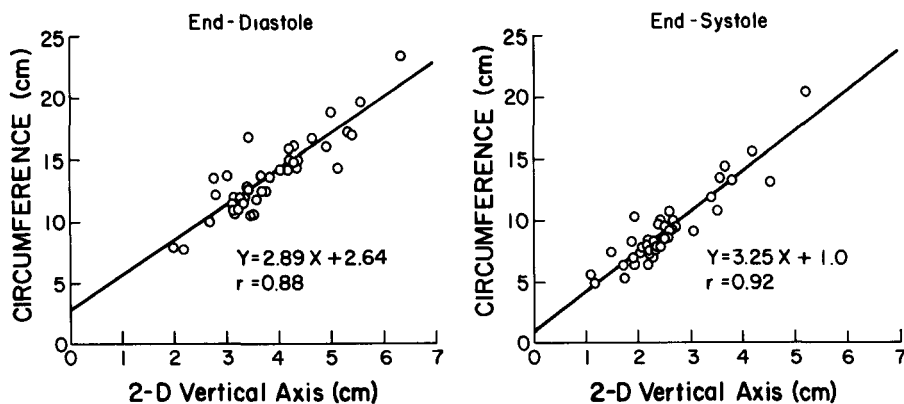
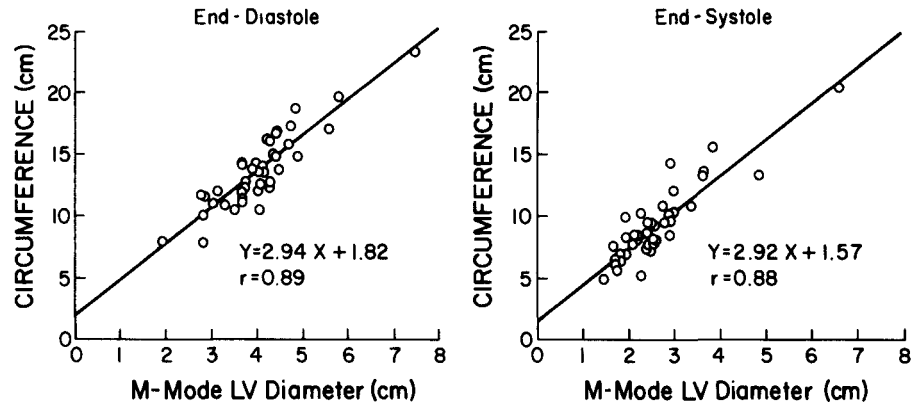


Figure 3. Circumference of the left ventricular sector image as a function of the vertical axis during end-diastole and end-systole. The linear regression lines, equations and correlation coefficients are shown.

Figure 4. Circumference of the left ventricular sector image as a function of the M-mode-derived left ventricular (LV) diameter during end-diastole and end-systole. The linear regression lines, equations and correlation coefficients are shown.



of two-dimensional Vcf revealed wide scatter of the data points.

In 14 young patients (6 normal, 3 with pressure overload, 4 with volume overload, 1 with primary myocardial disease), the M-mode Vcf calculations were almost identical to those derived from the two-dimensional echocardiograms in which left ventricular ejection time was obtained from the M-mode tracing, the difference between the two values being less than $\pm 10\%$ of the two-dimensional Vcf calculation. In 16 young patients (4 normal, 1 with pressure overload, 5 with volume overload, 6 with primary myocardial disease), the Vcf calculations by the two methods differed by $\pm 21\%$ or more of the two-dimensional Vcf estimation. In the remaining 10 patients (3 normal, 5 with pressure overload, 2 with volume overload), the difference between the Vcf calculations ranged from ± 10 to $\pm 20\%$ of the two-dimensional Vcf estimation. Thus, the differences between the two Vcf calculations did not appear to be greatly influenced by the basic cardiac disease although in six of the seven patients with primary myocardial disease the differences were quite large, ranging from $+23$ to -180% of the two-dimensional Vcf estimation.

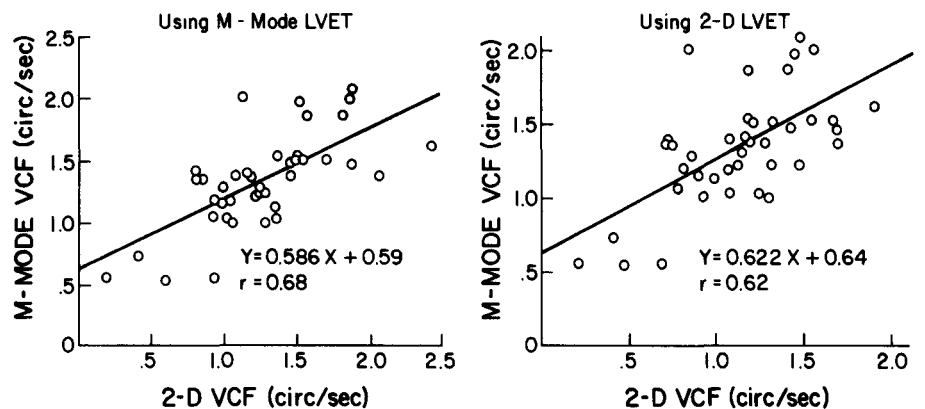
The Vcf derived by M-mode echocardiography averaged 1.34 ± 0.38 circ/s; the two-dimensional Vcf (utilizing M-mode left ventricular ejection time) was 1.25 ± 0.45 circ/s ($p = \text{NS}$). Corresponding values for two-dimensional Vcf

(utilizing two-dimensional left ventricular ejection time) were 1.13 ± 0.38 circ/s; these were significantly lower than the M-mode Vcf values ($p < 0.001$).

End-diastolic and end-systolic dimension/circumference ratios. A plot of the vertical axis/circumference ratio during diastole against the vertical axis/circumference ratio during systole and a similar plot using diameter/circumference ratios are shown in Figure 6; in both plots, poor correlations were observed. In addition, the regression equations relating the ratios during end-diastole to the corresponding ratios during end-systole significantly differed from the line of identity ($p < 0.001$).

In 18 young patients (6 normal, 4 with pressure overload, 6 with volume overload, 2 with primary myocardial disease), the differences between the end-diastolic and end-systolic vertical axis/circumference ratios were within $\pm 5\%$ of the end-diastolic values. In 12 children (4 normal, 2 with pressure overload, 2 with volume overload, 4 with primary myocardial disease), they were within 5 to 10%; in 10 children (3 normal, 3 with pressure overload, 3 with volume overload, 1 with primary myocardial disease), they were greater than $\pm 10\%$ of the end-diastolic values. In 14 children (6 normal, 3 with pressure overload, 4 with volume overload, 1 with primary myocardial disease), the differences between the end-diastolic and end-systolic diameter/circumference ratios were within $\pm 5\%$ of the end-diastolic

Figure 5. Comparison of circumferential fiber shortening velocity (Vcf) derived from M-mode echocardiogram with Vcf derived from two-dimensional echocardiogram using different left ventricular ejection times (LVET) for calculating the latter. **Left,** The left ventricular ejection time was obtained from the M-mode tracings. **Right,** The left ventricular ejection time was derived from the two-dimensional cine films. Linear regressions lines, equations and correlation coefficients are shown.



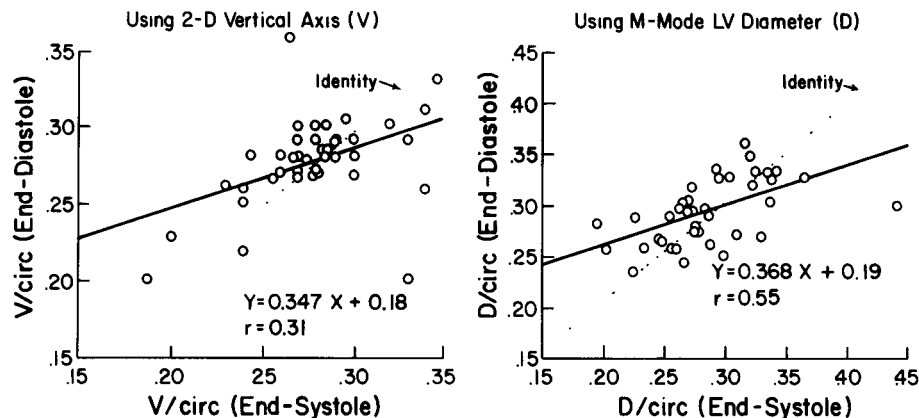


Figure 6. Comparison of the end-diastolic and end-systolic left ventricular minor axis/circumference (circ) ratios. **Left,** The vertical axis (V) derived from the two-dimensional sector image was used as the minor axis. **Right,** The left ventricular diameter (D) obtained from the M-mode tracing was used as the minor axis. Linear regression lines (solid) and lines of identity (dotted) are shown, as well as the regression equations and correlation coefficients.

values. In 10 children (2 normal, 2 with pressure overload, 3 with volume overload, 3 with primary myocardial disease), they were within 5 to 10%; and in 16 children (5 normal, 4 with pressure overload, 4 with volume overload, 3 with primary myocardial disease), they were greater than $\pm 10\%$ of the end-diastolic diameter/circumference ratios. Thus, the variation between the end-diastolic and end-systolic dimension/circumference ratios appeared to be unrelated to the left ventricular work load.

Discussion

Under basal conditions, the mean rate of circumferential fiber shortening is a relatively simple and satisfactory index of left ventricular performance even when valvular and myocardial defects coexist (9). Because the estimated velocity of circumferential change is divided by the end-diastolic circumference and expressed per unit of circumferential length, that is, as circumferences/s, the values can be utilized to compare the mechanics of cardiac performance among patients. Early methods for estimating mean circumferential fiber shortening velocity (Vcf) involved indicator-dilution techniques (10,11) and, later, cineangiography (9,12). In recent years, it has become a standard ultrasound determination. The advantages of the latter noninvasive approach are obvious.

Cooper et al. (3) compared the mean Vcf obtained by the ultrasound technique with those determined by cineangiography in which fractional shortening of the left ventricular minor axis was measured from the lateral angiograms. Although the observed values by the angiographic technique were higher than those by the ultrasound technique, good correlation ($r = 0.81$) was found. The ultrasound method was concordant with the angiographic method relative to normal or abnormal values in 96% of the patients studied. From these observations, the conclusion was made that the ultrasound method for mean Vcf estimation was valid. Kaye et al. (13) also found high correlation ($r = 0.91$) between angiographically-derived and echographically-derived mean Vcf in children. In con-

trast, Bhatt et al. (14) noted poor correlations between the echocardiographic and cineangiographic determinations of left ventricular fractional shortening and mean Vcf in children.

Validity of Vcf calculations. It is obvious, however, that both angiographic and echocardiographic methods for Vcf estimation merely evaluate fractional shortening of the left ventricular diameter at about the midequator; neither method determines ventricular circumference change. In both methods there is an assumption that dynamic changes in the circumference can be derived from corresponding changes in the minor axis diameter. This concept is mathematically valid if the cross-sectional area is completely circular (because circumference = diameter π) and ventricular contraction is completely synergic. It is also valid even if the cross section is noncircular, provided that its geometric shape remains constant throughout the cardiac cycle. Consequently, a fixed relation between minor axis and circumference exists to the extent that fractional shortening of the former should reflect a reduction of proportionate magnitude in the latter.

Our study utilized two-dimensional echocardiography to analyze changes in left ventricular circumference during systole. A 35 mm cine film of the sector image facilitated identification and tracing of the endocardial surface. Circumference was determined with computer assistance. The interobserver variability of the Vcf calculation by this method, averaging 6%, could be ascribed to dissimilar techniques in tracing the endocardial surfaces. Other factors include non-identical cardiac cycles analyzed and respiratory effects on ventricular preload or cardiac position (15,16). Ideally, the M-mode echocardiograms should have been obtained "simultaneously" with the two-dimensional sector studies utilizing the cursor in the sector scanner. However, the M-mode tracings from the latter are not of comparable quality with those obtained with the Hoffrel ultrasonoscope.

Evaluation of minor axis measurements. Despite the difference in approach used for determining left ventricular minor axis by the M-mode and two-dimensional methods, there was good correlation between the measurements by both. The former measured the endocardial septal to pos-

terior wall distance along the ultrasound trajectory which may or may not have traversed the "meridional center" of the ventricular cavity. In contrast, the vertical axis derived from the short-axis sector image represented the anteroposterior distance perpendicular to the plane of the mitral valve commissures at its midpoint. The explanation for the higher correlation coefficient at end-systole ($r = 0.88$) than at end-diastole ($r = 0.80$) is unclear. It may be related to the altered geometry of the sector image or to the change in spatial orientation, including rotational movement, of the left ventricle during systole relative to the fixed position and trajectory of the ultrasound transducer for the M-mode recordings.

Minor axis-circumference relations. The high correlations between left ventricular diameter obtained from the M-mode echocardiogram and circumference derived from the sector image, observed in end-diastole ($r = 0.89$) as well as in end-systole ($r = 0.88$), would argue for the usefulness of minor axis shortening as an indirect index of circumferential change during systole. However, unequivocal validation of this concept requires demonstration of a nearly constant relation between diameter and circumference throughout the cardiac cycle or at least during end-diastole as well as end-systole. Such a relation was observed in less than half of our patients and was unrelated to the left ventricular work load. When end-diastolic vertical axis/circumference ratio was plotted against end-systolic vertical axis/circumference ratio, the derived regression equation was clearly separate from the line of identity. A similar observation was made when end-diastolic diameter/circumference ratio was related to end-systolic diameter/circumference ratio (Fig. 6). Thus, it was not surprising to find only fair correlation ($r = 0.68$) between mean Vcf derived from the M-mode tracings and mean Vcf measured from the two-dimensional echocardiograms. We believe that our findings could be accounted for largely by the change in geometry of the left ventricular sector image during systole. As viewed in the short-axis projection, the end-systolic sector image is relatively more circular in configuration than the end-diastolic image.

Reliability of Vcf estimation. The reliability of Vcf estimation by the two-dimensional approach may be questioned because of the relatively slow filming rate of 30 frames/s (33 ms between sector images). Thus, it is possible that the true end-systolic image may have been missed and could have occurred between the immediately preceding cine frame and that showing onset of mitral valve opening. It is more likely, however, that the "end-systolic" sector image was obtained during isovolumic relaxation, which, in our experience, usually lasts 40 to 50 ms in children with a normal or abnormal heart, or even longer in those with cardiomyopathy. The mistiming of end-systole could have been by only several milliseconds during which time changes in left ventricular size are trivial, as observed in computer

plots of continuous left ventricular diameter curves (17). Because outward wall movement and slight increase in left ventricular cavity volume have been observed angiographically during isovolumic relaxation (18-20), it can be argued that our end-systolic circumference calculations may have been fortuitously high. However, our end-systolic diameters derived by M-mode echocardiography were obtained at the time of peak anterior excursion of the left ventricular posterior wall, which also occurs after aortic valve closure and just before mitral valve opening, that is, during isovolumic relaxation (21). Therefore, the timing of end-systole by both methods was comparable.

We do not wish to minimize the usefulness of mean Vcf derived by conventional M-mode echocardiography. It remains a useful index of left ventricular pump performance. However, the significant difference between end-diastolic and end-systolic left ventricular diameter/circumference relations, observed even in the absence of asynergic contraction abnormalities, strongly argues against extrapolating circumference change from minor axis shortening. The Vcf derived from M-mode echocardiography merely represents the mean shortening velocity of the minor axis, and no more than that. Although it could be argued that this is just a matter of semantics, we propose that it be given a different name, for example, mean velocity of minor axis shortening or mean velocity of fractional shortening.

References

- 1 Gault JH, Ross J Jr, Braunwald E. Contractile state of the left ventricle in man. *Circ Res* 1968;22:451-63.
- 2 Paraskos JA, Grossman W, Saltz S, Dalen JE, Dexter L. A non-invasive technique for the determination of velocity of circumferential fiber shortening in man. *Circ Res* 1971;29:610-5.
- 3 Cooper RH, O'Rourke RA, Karliner JS, Peterson KL, Leopold GR. Comparison of ultrasound and cineangiographic measurements of the mean rate of circumferential fiber shortening in man. *Circulation* 1972;46:914-23.
- 4 Goldberg SJ, Allen HD, Sahn DJ. Pediatric and Adolescent Echocardiography. Chicago: Year Book Medical, 1975:29-70.
- 5 Williams RG, Tucker CR. Echocardiographic Diagnosis of Congenital Heart Disease. Boston: Little, Brown, 1977:3-50.
- 6 Feigenbaum H. Echocardiography. 2nd ed. Philadelphia: Lea & Febiger, 1976:51-76.
- 7 Lester LA, Vitullo D, Sodt P, Hutcheon N, Arcilla R. An evaluation of the left atrial/aortic root ratio in children with ventricular septal defect. *Circulation* 1979;60:364-72.
- 8 Tajik AJ, Seward JB, Hagler DJ, Mair DD, Lie JT. Two-dimensional real-time ultrasonic imaging of the heart and great vessels: technique, image orientation, structure identification, and validation. *Mayo Clin Proc* 1978;53:271-303.
- 9 Karliner JS, Gault JH, Eckberg D, Mullins CB, Ross J Jr. Mean velocity of fiber shortening: a simplified measure of left ventricular myocardial contractility. *Circulation* 1971;44:323-33.

10. Gorlin R, Rolett EL, Yurchak PM, Elliott WC, Lane FJ, Levey RH. Left ventricular volume in man measured by thermodilution. *J Clin Invest* 1964;43:1203-21.
11. Wilcken DE. Load, work, and velocity of muscle shortening of the left ventricle in normal and abnormal human hearts. *J Clin Invest* 1965;44:1295-310.
12. Bristow JD, Van Zee BE, Judkins MP. Systolic and diastolic abnormalities of the left ventricle in coronary artery disease. *Circulation* 1970;42:219-28.
13. Kaye HH, Tynan M, Hunter S. Validity of echocardiographic estimates of left ventricular size and performance in infants and children. *Br Heart J* 1975;37:371-5.
14. Bhatt DR, Isabel-Jones JB, Villoria GJ, et al. Accuracy of echocardiography in assessing left ventricular dimensions and volume. *Circulation* 1978;57:699-707.
15. Lendrum BL, Mondkar AM, Harris JB, Smulevitz B, Carr I. Respiratory variation in echocardiographic dimensions of left and right ventricles in normal children: the role of the interventricular septum. *Pediatr Cardiol* 1979;1:39-45.
16. Brenner JJ, Waugh RA. Effect of phasic respiration on left ventricular dimension and performance in a normal population: an echocardiographic study. *Circulation* 1978;57:122-7.
17. Gibson DG, Brown D. Measurement of instantaneous left ventricular dimension and filling rate in man, using echocardiography. *Br Heart J* 1973;35:1141-9.
18. Alteri PI, Wilt SM, Leighton RF. Left ventricular wall motion during the isovolumic relaxation period. *Circulation* 1973;48:499-505.
19. Ruttley MS, Adams DF, Cohn PF, Abrams HL. Shape and volume changes during "isovolumetric relaxation" in normal and asynergic ventricles. *Circulation* 1974;50:306-16.
20. Gibson DG, Prewitt TA, Brown DJ. Analysis of left ventricular wall movement during isovolumic relaxation and its relation to coronary artery disease. *Br Heart J* 1976;38:1010-9.
21. Lacina SJ, Hutcheon N, Sodt PC, Rushhaupt DG, Thilenius OG, Arcilla RA. Which echo method for determining end-systolic dimension is accurate? (abstr). *Circulation* 1981;64(suppl IV):IV-168.